FE-analysis and experiment of optimized and standard link members of K-brace for passive seismic energy dissipation

Makoto Ohsaki[1], Junki Nozoe[1] and Hidekazu Watanabe[2]

[1]Department of Architecture, Hiroshima University
Kagamiyama 1-4-1, Higashi-Hiroshima 739-8527, Japan
{ohsaki, m125840}@hiroshima-u.ac.jp

[2] Department of Architecture, Hiroshima University
Currently, Materials and Structures Laboratories, Tokyo Institute of Technology,
Nagatsuda 4259, Midori, Yokohama 226-8503, Japan
watanabe@serc.titech.ac.jp

FE-model of link member of eccentrically braced frame

Passive control devices are widely used for reducing responses of building frames under earthquake excitation. An eccentrically braced frame (EBF) as shown in Fig. 1 dissipates seismic energy through plastic deformation of link members between the joints of beams and braces. The link member as shown in Fig. 2 has stiffeners in one side of the beam to avoid premature local buckling before dissipating enough energy.

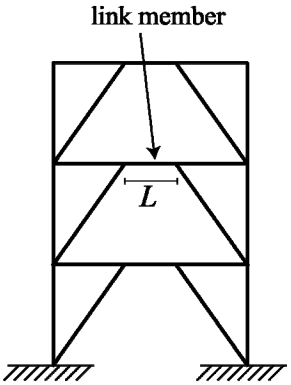

Fig. 1. An eccentrically braced frame.

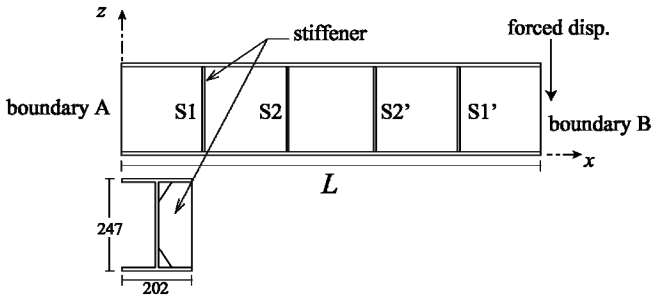

Fig. 2. Link member of EBF.

The beam is subjected to vertical cyclic displacement with fixed rotation at the right end (boundary B), while all displacement and rotation components are fixed at the left end (boundary A). The authors optimized the locations and stiffnesses of the stiffeners for maximizing the dissipated plastic strain energy before the maximum equivalent strain reaches the specified value [1]. A physical test has also been carried out for confirmation of performance [2]. The commercial software package ABAQUS Ver. 6.11 was used, and the optimal solutions of a discretized combinatorial problem was obtained by a heuristic algorithm called tabu search. In this study, we carry out detailed finite element (FE) analysis for the standard and optimal models as shown in Fig. 3(a) and (b), respectively, using an FE analysis software called ADVENTURECluster [3].

All plates including flange, web, and stiffener are discretized into two layers of hexahedral elements as shown in Fig. 4, which is generated using ABAQUS CAE. The non-conforming linear interpolation element is used. For the standard model, the number of elements is 38234 including 1048 rigid bars connecting the nodes on boundaries and the control nodes at their centers. The number of nodes and degrees of freedom are 61110 and 184128, respectively.

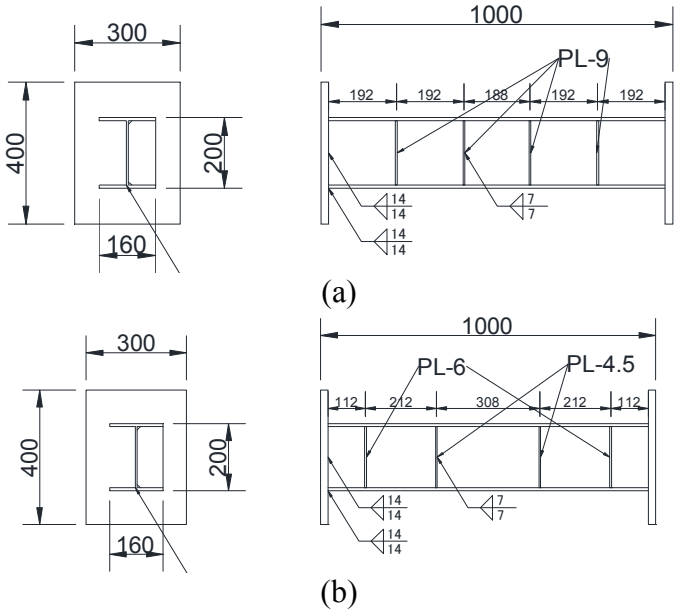

Fig. 3. Details of link members; (a) standard model, (b) optimal model.

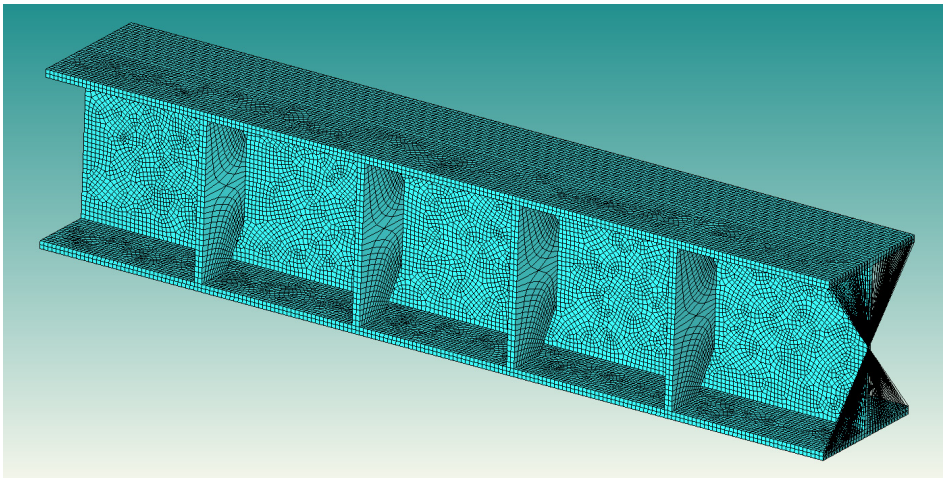

Fig. 4. FE mesh for standard model.

The material properties including Young's modulus are identified from the results of uniaxial coupon tests. The piecewise linear isotropic/kinematic hardening model in Ref. [5] is used, and the ratio of isotropic hardening that cannot be determined from the uniaxial test is assigned as 2/3, which is the same as Ref. [4].

Results of FE-analysis

Fig. 5(a) and (b) show the relations between the vertical displacement and reaction force at the control nodes for standard and optimal models, respectively, while the left end is fixed. The reaction obtained by FE-analysis is plotted in red line, which has smaller absolute value than the experimental result in blue line. It should be noted that the initial stiffness of numerical result is larger than that of experiment. Therefore, rotational springs of 4.0×10^4MNm/rad are placed around y-axis at the control nodes in both boundaries to incorporate the flexibility of loading equipment.

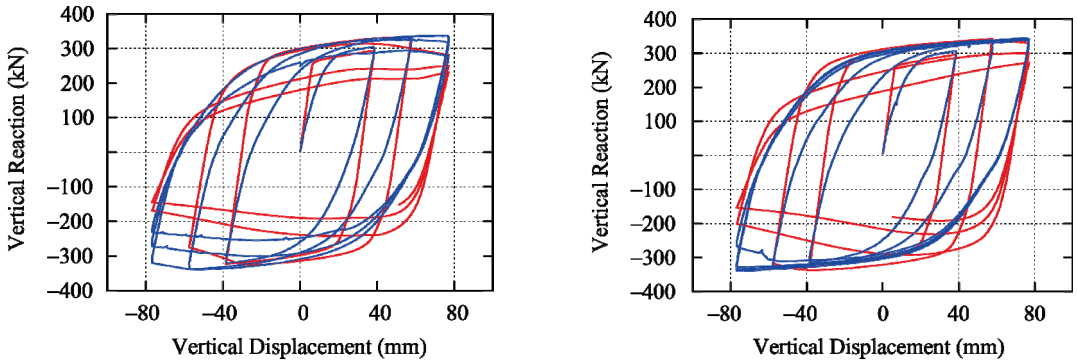

Fig. 4. Relation between vertical displacement and reaction for fixed rotation at the control node; red line: analysis, blue line: experiment, (a) standard model, (b) optimal model.

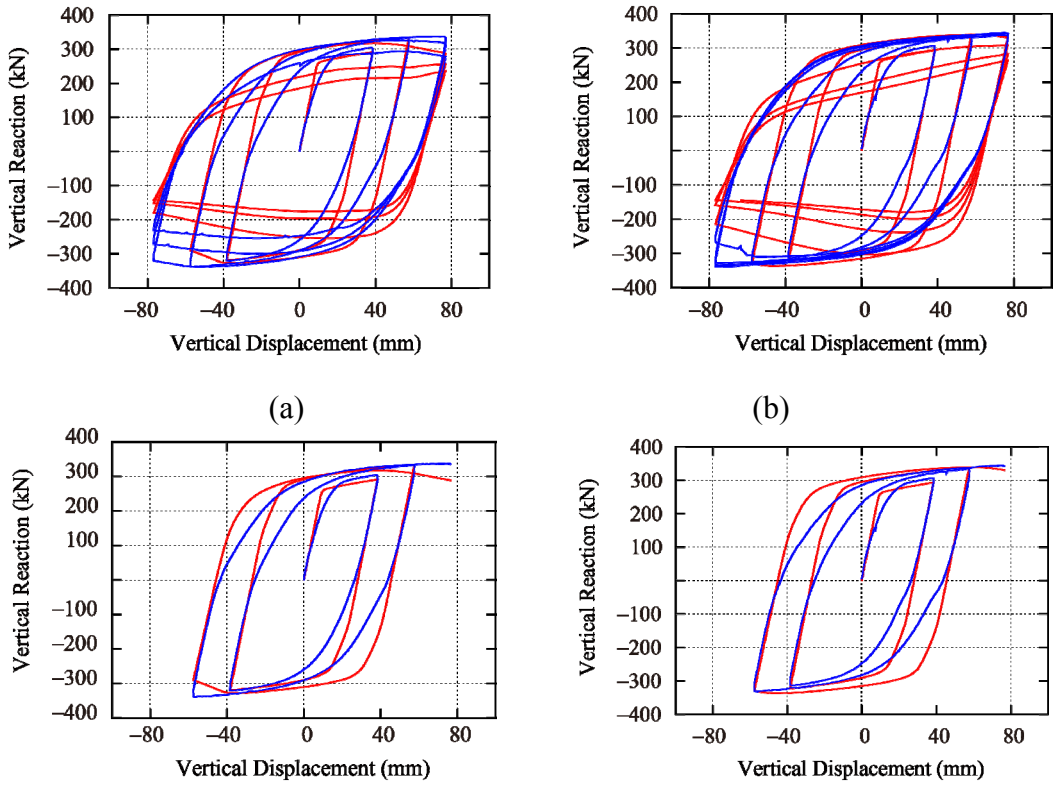

Fig. 5. Relation between vertical displacement and reaction with rotational springs at the control nodes; red line: analysis, blue line: experiment, (a) and (c) standard model, (b) and (d) optimal model.

Relations between the vertical displacement and reaction force at the control nodes of the models with rotational spring are plotted in Fig. 5, where (a) and (b) are standard and optimal models, respectively, and the relations before reaching the third maximum displacement are plotted in (c) and (d). It is observed from these figures that the load-displacement can be accurately traced until the third cycle before buckling occurs in the flange. The fifference in the initial stiffness has small effect on deformation in the subsequent cycles. Strength of the standard model degrades more rapidly than the optimal model.

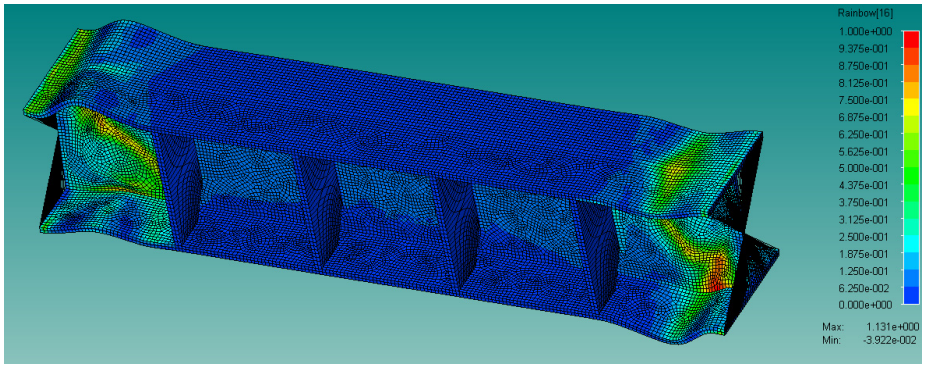

(a)

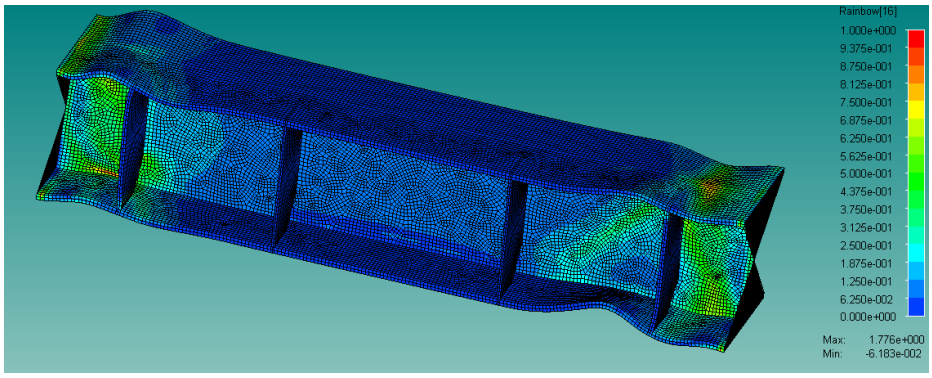

(b)

Fig. 6. Equivalent plastic strain at fourth maximum deformation; (a) standard model, (b) optimal model.

Fig. 6(a) and (b) show the distribution of equivalent plastic strain at the fourth maximum deformation of the standard model and optimal model, respectively. It can be observed from these figures that accumulation of plastic strain in the web near the right end is alleviated and the flange buckling moves to the center by optimizing the locations of stiffeners.

Acknowledgement:
This work is partly supported by Grant-in-Aid for Scientific Research of JSPS (No. 23360248).

References

[1] M. Ohsaki and T. Nakajima, Optimization of link member of eccentrically braced frames for maximum energy dissipation, J. Constr. Steel Res., Vol. 75, pp. 38–44, 2012.
[2] H. Watanabe, M. Ohsaki and J. Nozoe, An experimental study on hysteresis characteristics of optimally-designed link member of eccentrically braced frames, Annual Meeting of Architectural Inst. Japan, Hokkaido, Paper No. 22518, 2013. (in Japanese)
[3] Allied Engineering Corporation. http://www.alde.co.jp/english/advc/index.html.
[4] M. Ohsaki, J. Y. Zhang, T. Miyamura, A heuristic algorithm for parameter identification of steel materials under asymmetric cyclic elastoplastic deformation, Proc. 7th China-Japan-Korea Joint Symposium on Optimization of Structural and Mechanical Systems (CJK-OSM7), Huangshan, China; 2012.